# Composition and Temperature Dependence of Monomer Friction in Polystyrene/Poly(methyl methacrylate) Matrices

**Jodi M. Milhaupt† and Timothy P. Lodge***

*Department of Chemistry and Department of Chemical Engineering & Materials Science, University of Minnesota, Minneapolis, Minnesota 55455*

**Steven D. Smith and Mark W. Hamersky**

*The Procter & Gamble Company, Miami Valley Laboratories, Cincinnati, Ohio 45247*

*Received February 12, 2001*

ABSTRACT: The composition ($\phi$) and temperature dependence ($T$) of the monomeric friction factor ($\zeta$) has been examined for styrene (S) and methyl methacrylate (MMA) in five SMMA diblock copolymers and the corresponding homopolymers. In all cases the degree of polymerization was approximately 150, sufficiently low to ensure that the chain dynamics follow the Rouse model and that the copolymers are far above the order−disorder transition. The five diblock copolymers had styrene compositions of 91, 70, 39, 19, and 9 wt %. Values of an effective friction factor, $\zeta_{eff}$, were obtained from measurements of the steady flow viscosity via the Rouse model, whereby $\zeta_{eff}$ represents an average over the S and MMA contributions. Values of the component friction factors, $\zeta_{PS}$ and $\zeta_{PMMA}$, were extracted from forced Rayleigh scattering tracer diffusion measurements of dye-labeled PS, PMMA, and SMMA chains. In accord with previous studies, $\zeta_{PMMA}$ in pure PMMA is significantly greater than $\zeta_{PS}$ in pure PS, whether compared at equal $T$ or equal $T - T_g$, an effect attributable to specific details of local relaxation in PMMA. This difference between $\zeta_{PMMA}$ and $\zeta_{PS}$ persists in a common SMMA matrix, an effect which can be quantitatively accounted for by the recently introduced concept of self-concentration. The values of $\zeta_{eff}$ increase monotonically with MMA content at fixed $T$ and with decreasing $T$ at fixed $\phi$. The $\phi$ dependence of $\zeta_{eff}$ is consistent with both "Rouse" and "Arrhenius" mixing rules, utilizing the pure component friction factors as input. The $T$ dependence of $\zeta_{eff}$ follows the standard Williams−Landel−Ferry relation, but the data for different $\phi$ do not collapse to a single curve when plotted against $T - T_g$. In this respect, the PS/PMMA system is more complicated than the previously studied PS/polyisoprene system.

## Introduction

There has recently been a great deal of interest in understanding the composition ($\phi$) and temperature ($T$) dependence of the rate of segmental relaxation in polymer mixtures.[1−17] This fundamental property may be conveniently discussed in terms of the monomeric friction factor, $\zeta(\phi,T)$.[18] Utilizing current molecular theories, based for example on the reptation model, it is possible to make quantitative predictions for the dynamic properties of homopolymer melts, provided one has access to the temperature dependence of $\zeta$. However, in mixtures the analogous predictions are not yet reliable. Given that $\zeta$ can vary by several orders of magnitude over relatively modest temperature intervals above the glass transition temperature in simple homopolymers, it is not surprising that simple "mixing rules" have the potential to be substantially in error when applied to blends or copolymers. Experiments on miscible blends have borne this out; the behavior of $\zeta(\phi,T)$ is often remarkably complicated. Two general strategies for the extraction of information about $\zeta(\phi,T)$ have been employed. One relies on techniques that can sense local dynamics directly, such as dielectric relaxation,[8,10,13] NMR,[2,9] fluorescence anisotropy,[14] and neutron spin echo.[15] The second follows chain dynamics, for example through diffusion,[1,5,6,19] rheology,[3,12,20] or rheooptics,[7] and extracts $\zeta(\phi,T)$ via established dynamic models. Both approaches have great utility; in this work we emphasize the latter, and especially chain diffusion, because it provides the most direct route to the contribution made by each component to the overall long-time dynamics of the mixture.

Immiscible polymer pairs are also of interest in this context. Spinodal decomposition of blends, block copolymer diffusion, and viscoelasticity and processing of multicomponent polymers all represent situations in which the mobility of one component in an environment rich in other components plays a fundamental role. In this case direct measurements on blends are not straightforward, because of phase separation. The expedient of reducing molecular weight until miscibility is achieved is not often practical, because for typical pairs of interest the resulting components would be essentially oligomers. For such short chains the local dynamics and chain dynamics are not easily resolved, and chain end effects play a disproportionate role. Consequently, we have developed an alternative approach using disordered multiblock copolymers.[21,22] By reducing the average block length the order−disorder transition temperature can be suppressed well below the experimentally interesting range, while the number of blocks can be increased to maintain a suitable total chain length. The overall composition of the matrix can be adjusted by varying the relative block lengths within the copolymer and by blending copolymers of different composition. For example, in the polystyrene/polyisoprene (PS/PI) system four tetrablock copolymers with total molecular weights of approximately 12 000 and styrene compositions of 0.23, 0.42, 0.60, and 0.80 by volume were employed. Measurements of the self-diffusion and viscosity of these SISI copolymers, and corresponding homopolymers,

† Department of Chemistry.
* Author for correspondence: e-mail lodge@chem.umn.edu.

10.1021/ma010265d CCC: $20.00 © 2001 American Chemical Society
Published on Web 06/19/2001

provided access to an *effective* friction factor $\zeta_{eff}(\phi,T)$ defined by applying the Rouse model and assuming that each monomer was equivalent.[21] Then, measurements of tracer diffusion of a PS homopolymer, a PI homopolymer, and an SI diblock in these matrices enabled resolution of the *component* friction factors $\zeta_{PS}(\phi,T)$ and $\zeta_{PI}(\phi,T)$. The results were remarkable in their simplicity; to a good approximation $\zeta_{PS}(\phi,T) \approx \zeta_{PI}(\phi,T) \approx \zeta_{eff}(\phi,T)$ in all cases and depended only on the temperature interval above the matrix glass transition temperature, $T_g$.[22] Thus, despite the huge difference in their respective $T_g$s, PS and PI have essentially equal friction factors in a common matrix.

In this work we extend this approach to PS/poly(methyl methacrylate) (PMMA). This pair is intriguing because the respective friction factors in the pure homopolymers differ by ca. 2 orders of magnitude at a given distance above $T_g$, for reasons that remain obscure; PMMA has the larger $\zeta$.[18] On the other hand, PS and PMMA have rather similar values of $T_g$, in contrast to PS/PI. Furthermore, pioneering measurements by Green have shown that this difference in friction factors persists for tracer diffusion of an SMMA diblock diffusing in a PS melt; the resulting $\zeta_{eff}(T)$ resembles PMMA in PMMA, even though the matrix is pure PS.[23] For PS/PMMA the Flory−Huggins interaction parameter is smaller than in PS/PI, and consequently diblocks with molecular weights of ca. 15 000 are far above the order−disorder transition. We report results for $\zeta_{eff}(\phi,T)$ for five SMMA diblocks of varying composition from viscosity and diffusion measurements. Furthermore, the component friction factors are extracted from measurements of PS, PMMA, and SMMA diblock tracer diffusion. The dependence of the various friction factors on the matrix and tracer composition are discussed in terms of simple mixing rules and in comparison to those for the PS/PI system. The temperature dependence is also discussed, with particular attention to the effect of the so-called self-concentration, as recently described.[17]

## Experimental Section

**Materials.** The reagents were purified as follows. Cyclohexane (Phillips Petroleum) was stirred over sulfuric acid for 1 week and then distilled from calcium hydride. Tetrahydrofuran (THF, Fisher) was distilled from a sodium benzophenone ketal. Dibutylmagnesium and *sec*-butyllithium were used as received (Lithium Corporation of America), as was triethylaluminum (Aldrich). Methyl methacrylate (Aldrich) was purified by treatment with triethylaluminum and was subsequently distilled under vacuum.[24] Styrene (Aldrich) was purified by passing through an alumina column to remove inhibitors, then titrating impurities with dibutylmagnesium, and finally passing through an activated alumina column to remove magnesium salts. 1,1-Diphenylethylene (Kodak) was purified by the reaction of impurities with *sec*-butyllithium followed by vacuum distillation. Benzaldehyde (Aldrich) was purified by stirring over calcium hydride for 24 h followed by vacuum distillation.

Block copolymer and homopolymer synthesis was carried out in round-bottom flasks, equipped with septa, using magnetic stirring under a nitrogen atmosphere. Typically 20% solutions of styrene in cyclohexane and 1 vol % THF were prepared. The styrene blocks were initiated with *sec*-butyllithium and allowed to react for 15 min, at which time further purified styrene monomers were added to produce the desired block lengths. The polystyryllithium chains were capped with 1,1-diphenylethylene to produce a more sterically hindered carbanion. This carbanion has been shown to initiate methyl methacrylate polymerization without the undesired addition to the carbonyl that occurs with styryllithium.[25] The reactions were diluted with purified THF such that they contained minimally 75 vol % THF and were then cooled to −78 °C. Purified methyl methacrylate was then added dropwise to the polymerization. It is necessary to add the monomer slowly to maintain the reaction temperature below −60 °C to avoid side reactions. The methyl methacrylate polymerization is extremely rapid and is essentially complete within 60 s under these conditions. Termination of the chain ends with a hydroxyl functionality was achieved by reaction of the living anions with a slight excess of benzaldehyde. The polymers were precipitated into a 10-fold excess of acidic methanol and vacuum-dried. Soxhlet extraction with cyclohexane was found to be efficient at removing any free polystyrene homopolymer resulting from termination of the first block.

**Table 1. Characterization of Polymers Used**

| polymer | $M_n$, kg/mol | $M_w/M_n$ | $W_{PS}$ |
|---|---|---|---|
| PS-13 | 13.$_0$ | 1.06 | 1.00 |
| PS-13.5 | 13.$_5$ | 1.06 | 1.00 |
| SMMA-91 | 16.$_0$ | 1.01 | 0.90 |
| SMMA-70 | 15.$_7$ | 1.01 | 0.68 |
| SMMA-39 | 14.$_8$ | 1.02 | 0.37 |
| SMMA-19 | 15.$_7$ | 1.01 | 0.18 |
| SMMA-9 | 16.$_5$ | 1.03 | 0.087 |
| PMMA-12 | 11.$_9$ | 1.03 | 0.00 |

**Characterization.** Molecular weights and molecular weight distributions were determined by size exclusion chromatography with Ultrastyragel columns of 500, $10^3$, $10^4$, and $10^5$ Å porosities in THF. Compositions were determined by $^1$H NMR analysis. Molecular weights of all five SMMA diblock copolymers and the PS and PMMA copolymers are listed in Table 1, along with the polydispersity and composition. The homopolymers are designated PS-13 and PMMA-12, where the numerical suffix refers to the molecular weight in kg/mol. The diblocks are denoted SMMA-*xx*, where *xx* refers to the styrene composition by volume percent; the volume fraction of PS within a chain will be designated *f*. These were calculated from the experimentally determined mole fractions assuming additivity of volumes and densities of 1.05 and 1.15 g/mL for PS and PMMA, respectively. The volume fraction of PS within the matrix will be designated $\phi$; $f$ and $\phi$ can be different in the case of tracer diffusion.

**Labeling.** Both PMMA-12 and SMMA-39 were labeled with a two-step procedure similar to that used by Faldi.[26] First, an alcohol functionality was added randomly along each chain through reaction of the methyl ester side groups with ethanolamine. A 2:1 molar ratio of freshly distilled ethanolamine (Aldrich) to polymer was added to a solution of 1,4-diazabicyclo[2.2.2]octane (Aldrich) in dry dimethylformamide (Aldrich) to make a polymer solution with a concentration between 0.05 and 0.1 g/mL. The solution was refluxed for 4 h under nitrogen. After cooling the reaction mixture was filtered with an 0.45 $\mu$m syringe filter into a 40 mL methanol:30 mL water:10 mL hydrochloric acid solution to precipitate the functionalized polymer. The polymer was recovered, rinsed with water until a neutral pH was achieved, and dried under vacuum for 1−2 days.

The resulting functionalized polymers were labeled through a condensation reaction with the photochromic dye 4′-(*N*,*N*-dimethylamino)-2-nitrostilbene-4-carboxylic acid (ONS−COOH). The synthesis of ONS−COOH has been described previously.[27] For 0.2 g of polymer, a 5 times molar excess of ONS−COOH and the polymer were dissolved in 20 mL of dichloromethane. The dichloromethane was purified by stirring on calcium hydride overnight and vacuum distillation. Once the polymer was completely dissolved, approximately 0.08 g each of dicyclohexylcarbodiimide (DCC) and (dimethylamino)pyridine were added to the reaction solution. The solution was refluxed under nitrogen for 1 week. The PMMA-12* was dissolved in tetrahydrofuran and purified through successive reprecipitations by slow addition of a 1:1 mixture of water:methanol (SMMA-39* was purified by addition of pure methanol), where the asterisk denotes the labeled product. Removal of the excess free dye was verified with SEC using refractive index (Wyatt

Corporation Optilab) and ultraviolet detection (Gilson model 166).

Two labeled polystyrene homopolymers have been used in this study. The precursor to PS-13* was obtained from Pressure Chemical (Lot 30420) and has been used in several previous studies.[21,22,27] The labeling was accomplished through aminomethylation of a small fraction of the phenyl rings and a subsequent condensation reaction with ONS−COOH.[27] The second polystyrene homopolymer tracer, PS-13.5*, was synthesized as outlined above, where the anionic polymerization was terminated with benzaldehyde leaving a benzylic alcohol. This alcohol was reacted via a condensation reaction with ONS−COOH and a large excess of DCC. The mixture was sealed under nitrogen in a pressure reaction flask (Chemglass) and allowed to react for 5 days at temperatures between 60 and 75 °C.

**Differential Scanning Calorimetry.** All differential scanning calorimetry (DSC) measurements were performed on a Perkin-Elmer DSC7 which was calibrated with an indium standard. Each 7−15 mg specimen was annealed overnight under vacuum at 150 °C prior to sealing within an aluminum sample pan. This was necessary to remove any water or other solvents absorbed within the polymers. A consistent protocol of heating and cooling steps was followed during the measurement. The sample was first heated to 160 °C where the temperature was held for 10 min. Then the sample was cooled at 10 °C/min to 30 °C where it was held for 2 min. The glass transition temperature was extracted from the subsequent heating from 30 to 160 °C at 10 °C/min. The glass transition temperature was defined as the temperature at half of the change in the heat flow. The average of the results from two specimens was used to determine the DSC glass transition temperature.

**Rheology.** The shear moduli were measured as a function of temperature and frequency on a Rheometrics ARES rheometer using the parallel plate geometry. Each sample was heated to 130−140 °C under vacuum, pressed into a 7.94 mm diameter, 1 mm thick disk, and loaded into the rheometer. The samples were loaded at room temperature and heated to 180 °C. The gap was approximately 1 mm and was adjusted to account for the expansion (or retraction) of the plates with temperature (0.0024 mm/°C). The isothermal frequency sweeps were performed first. The strain amplitude was set to optimize the torque while ensuring that the measurements were made in the linear viscoelastic regime, and the elastic and loss moduli, $G'$ and $G''$, were measured at frequencies, $\omega$, between 100 and 0.01 rad/s. The zero-shear viscosity, $\eta$, was taken as the limiting value of $G''/\omega$ as $\omega \rightarrow 0$; this was calculated by averaging 4−6 data points in the low-frequency plateau. Following the frequency sweeps, the samples were cooled below $T_g$, and $G'$ and $G''$ were measured as a function of temperature with a heating rate of 2 °C/min and a constant strain amplitude (0.1%) and frequency (1 rad/s).

**Forced Rayleigh Scattering.** The tracer diffusion coefficient has been measured using forced Rayleigh scattering in the amplitude mode; details of this technique have been discussed previously.[22,26] The resulting decays were fit to triple-exponential functions

$$I(t) = [A_1 \exp(-t/\tau_1) - A_2 \exp(-t/\tau_2) + A_3 \exp(-t/\tau_3)]^2 + C \quad (1)$$

where $A_1$, $A_2$, and $A_3$ are the amplitudes of the modes with the relaxation times $\tau_1$, $\tau_2$, and $\tau_3$, respectively, and $C$ is the incoherent baseline. Only for the slowest mode was the relaxation time dependent on the grating spacing, $d$, and thus it was from this mode that the diffusion coefficient was determined (see also Figure 6 and associated discussion). The remaining modes are independent of $d^2$, only weakly dependent on temperature, and have been described previously.[22] The complexity of the photoisomerization reaction is implicated in such decays.[28]

The FRS samples were prepared by codissolving 3.5−6.0 wt % of the ONS-labeled tracer and matrix in THF or dichloromethane, filtering the solutions with an 0.45 $\mu$m Nalgene syringe filter, removing excess solvent, and precipitating in methanol or methanol/water solutions. The polymer was dried under vacuum for 1−2 days and then placed into one-half of a sample cell comprising a glass window adhered to an annular aluminum spacer. The sample was then heated under vacuum to between 120 and 150 °C until a constant sample mass was achieved. A second glass disk was sealed unto the sample cell under an argon environment. Before FRS measurements were made the samples were annealed between 150 and 170 °C for several days, until the polymer no longer flowed within the sample cells.

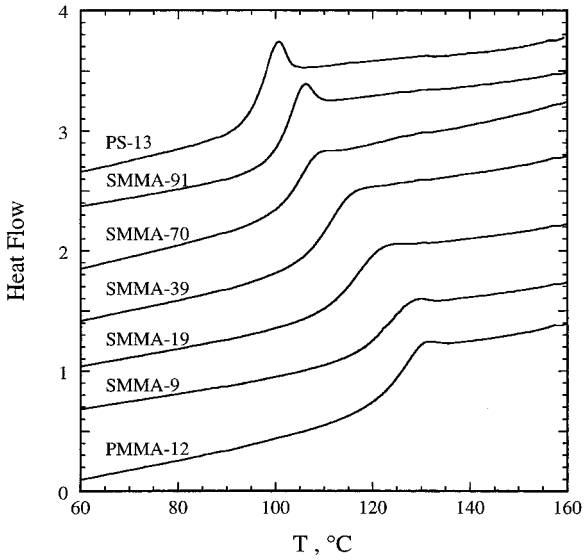


**Figure 1.** Heat flow as a function of temperature for the indicated polymers. The traces were obtained upon heating at 10 °C/min and have been displaced vertically for clarity.

## Results

The remainder of the paper is organized as follows. In this section we present the glass transition temperatures, the zero-shear viscosities, and the tracer diffusion coefficients. The extraction of monomeric friction factors and their dependence on temperature, matrix composition, and tracer composition will be described in the Discussion section.

**Glass Transition.** Representative DSC traces are shown in Figure 1. The glass transition temperature increases steadily with increasing MMA content, as expected. The breadth of the transition also increases as the MMA content first increases, which is consistent with previous results on many blends. However, it is clear that the transition is significantly broader even for pure PMMA than for pure PS or SMMA-91.

Rheological characterization of the transition is illustrated in Figure 2, where the peak in the loss modulus is emphasized. The moduli for the various polymers, $G''$, are normalized by the respective peak values, $G''_{max}$, and plotted against temperature difference from $T_g$; the value of $T_g$ is defined by the peak location. This format emphasizes the breadth of the transition, and the trends discerned in Figure 1 are also clearly evident here. In particular, the width of the transition increases monotonically with MMA content and is broadest for PMMA-12. This interesting result is probably attributable to the inevitable stereochemical distributions, given the known sensitivity of $T_g$ in PMMA to microstructure.[29] In these polymers the fraction of syndiotactic triads decreased monotonically from 0.78 in PMMA-12 down to 0.71 in SMMA-91.

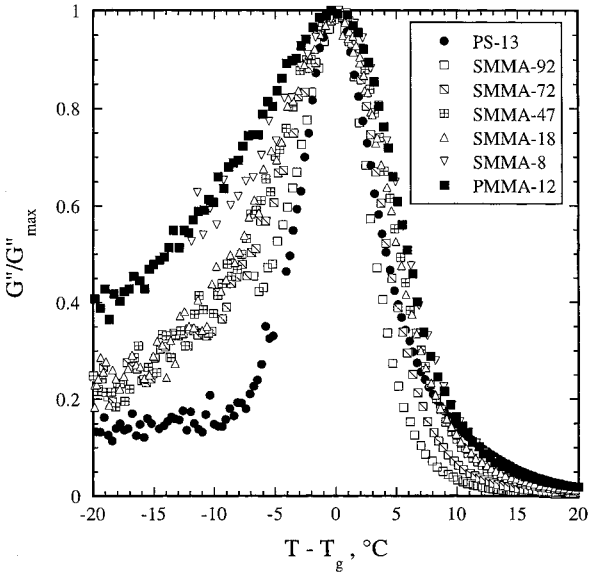


**Figure 2.** Normalized loss modulus $G''/G''_{max}$ for the indicated polymers as a function of temperature interval from $T_g$, where $T_g$ is identified with the maximum in $G''$; data were obtained at 1 rad/s while heating at 2 °C/min.

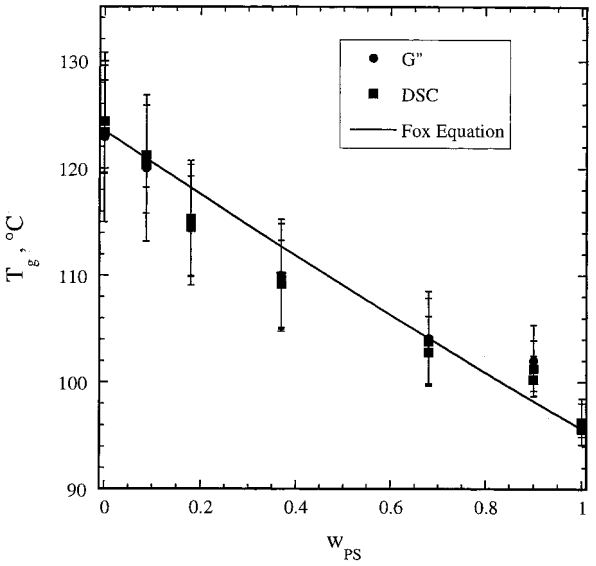


**Figure 3.** Glass transition temperatures as a function of weight fraction of polystyrene as determined by both DSC and $G''$; the solid line represents the Fox equation.

The resulting values of $T_g$ are plotted in Figure 3 and also listed in Table 2. The values from DSC and rheology are in excellent agreement. The composition dependence is compared with the Fox equation[30] in Figure 3:

$$\frac{1}{T_g} = \frac{w_{PS}}{T_{g,PS}} + \frac{w_{PMMA}}{T_{g,PMMA}} \qquad (2)$$

where $w$ is a weight fraction. The correspondence is reasonable, albeit not exact; the data indicate a more complicated composition dependence, even when allowing for the breadth of the transition (the error bars in Figure 3).

**Viscosity.** The linear viscoelastic properties of the MMA-containing polymers are shown in Figure 4. Time−temperature superposition has been used to obtain master curves, with a reference temperature of 160 °C. The superposition works well, which supports the inference that these copolymers are well into the disordered state. However, it must be noted that the range of temperature is relatively small, and most of the data fall in the terminal regime, where the superposition is anticipated. There is also no evidence of the large-amplitude composition fluctuations generally seen in close proximity to the ordering transition.[31,32] There is no hint of entanglement effects in any of the data, i.e., there is no clear maximum in $G''$ with frequency; this also is expected given the low molecular weights employed and the known values of $M_c$ for PS and PMMA (31 000 and 30 000, respectively[33]). This observation provides the justification for utilizing the Rouse model to extract the monomeric friction factors, as will be described in the Discussion section.

**Table 2. Glass Transition Temperatures**

| $W_{PS}$ | $T_g$, °C (DSC) | $T_g$, °C ($G''$) | $T_g$, °C (av) |
|---|---|---|---|
| 1.00 | 95.9 | | 95.8 |
| 0.90 | 100.7 | 102.0 | 101.3 |
| 0.68 | 103.3 | 104.1 | 103.7 |
| 0.37 | 109.6 | 110.0 | 109.8 |
| 0.18 | 114.9 | 114.7 | 114.8 |
| 0.087 | 120.7 | 120.0 | 120.3 |
| 0.00 | 123.8 | 122.9 | 123.4 |

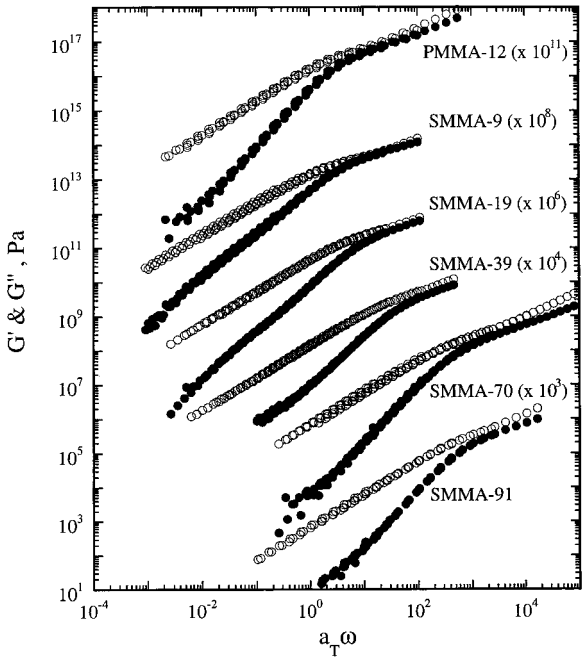


**Figure 4.** Dynamic shear moduli $G'$ (●) and $G''$ (○) as functions of the reduced frequency, with a reference temperature of 160 °C. Vertical displacements are identified on the plot.

The steady shear viscosity, $\eta$, extracted from the low-frequency limit of $G''$, is plotted as a function of temperature in Figure 5 for the two homopolymers and the five copolymers. The smooth curves represent fits to the WLF equation[18]

$$\log \frac{\eta(T)}{\eta(T_{ref})} = \frac{-C_1(T - T_{ref})}{C_2 + (T - T_{ref})} \qquad (3)$$

utilizing 160 °C as the reference temperature; the parameter values are listed in Table 3. In all cases the temperature dependence is strong, due to the proximity to the glass transition, and the temperature dependence appears to vary little with composition. The magnitude

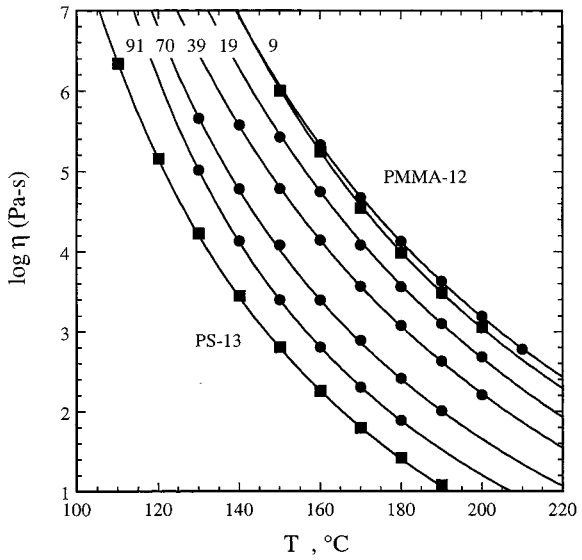


**Figure 5.** Semilogarithmic plot of the zero-shear viscosity as a function of temperature for the indicated homopolymers (■) and copolymers (●). Solid lines represent WLF fits.

**Table 3. WLF Fits to the Steady-Shear Viscosity with a Reference Temperature of 160 °C**

| polymer | $C_1$ | $C_2$, °C | log $\eta(T_{ref})$ |
|---|---|---|---|
| PS-13 | 6.26 | 126.5 | 2.260 |
| SMMA-91 | 6.16 | 113.7 | 2.807 |
| SMMA-70 | 7.19 | 124.9 | 3.398 |
| SMMA-39 | 8.90 | 145.3 | 4.145 |
| SMMA-19 | 9.79 | 148.1 | 4.750 |
| SMMA-9 | 9.79 | 142.6 | 5.328 |
| PMMA-12 | 9.40 | 130.6 | 5.248 |

of the viscosity at fixed temperature increases monotonically with increasing MMA content, except for SMMA-9 compared with PMMA-12. However, this apparent anomaly is a simple consequence of the difference in total molecular weight (see Table 1).

**Tracer Diffusion.** As noted in the Experimental Section, the FRS decays were not fully described by single-exponential decays. The triple-exponential function (eq 2) was always successful in fitting the complete decay. The complexity arises only at rather short times (typically before 1 s) and is attributable to complementary gratings ($A_1$ and $A_2$ have opposite sign). This probably reflects the photochemistry of ONS, in which there is a long-lived intermediate in the photoisomerization.[28] However, the associated decay times are independent of grating spacing, $d$, and thus the phenomenon does not involve diffusion. In contrast, the third mode has a decay time $\tau$ that increases linearly with $d^2$, and this decay dominates the long-time response. An example is shown in Figure 6, for PMMA-12* diffusing in SMMA-19. Decays are shown for three values of $d^2$, along with the associated fits, at a temperature of 166 °C. The dependence of $\tau$ on $d^2$ at various temperatures is shown in the inset. Consequently, we are confident that, despite the complexity of the decays, the diffusion coefficient of the tracer, $D$, can be determined reliably.

Figure 7 presents the measured diffusivities for the three tracers as a function of temperature, in all the matrices in which the tracer could be dissolved. For example, in the top panel $D$ for PMMA-12* in SMMA-73, SMMA-49, SMMA-19, SMMA-9, and PMMA-12 is

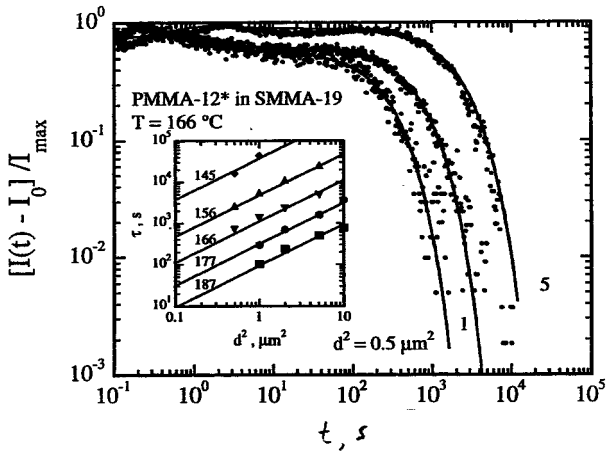


**Figure 6.** Normalized FRS decays for PMMA-12* in SMMA-19 at 166 °C for three grating spacings. The smooth curves represent fits to eq 1. The inset shows the decay time from the slowest mode as a function of grating spacing squared for the indicated temperatures.

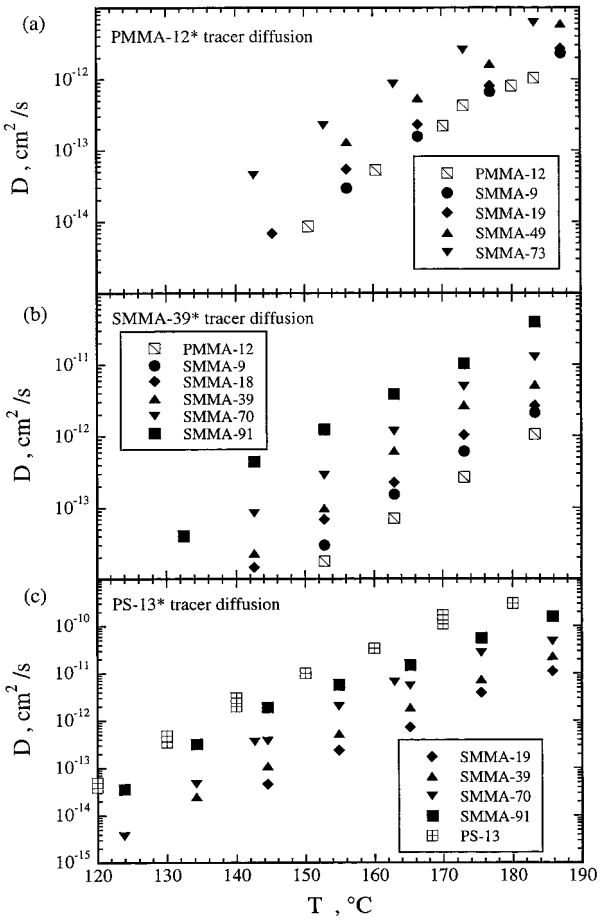


**Figure 7.** Diffusion coefficients as a function of temperature for (a) PMMA-12*, (b) SMMA-39*, and (c) PS-13* tracer diffusion in the indicated matrices.

shown; PMMA-12* could not be homogeneously dispersed in either SMMA-91 or PS-13. In each panel one data set corresponds to self-diffusion, i.e., equivalent tracer and matrix. In all cases $D$ increases monotonically with temperature in any given matrix and increases with styrene content of the matrix at fixed temperature. Furthermore, for any given matrix and temperature, the diffusivity increases with styrene content of the tracer.

## Discussion

The monomeric friction factor $\zeta$ provides a convenient framework in which to examine in detail the composition and temperature dependence of local dynamics. For the molecular weights employed here, the Rouse model should provide a good description of chain dynamics and can be used to extract $\zeta$ directly. Specifically, the Rouse model gives[18,34]

$$\zeta_{\text{eff}} = \frac{36M_0}{N_a \rho N b^2}\eta \tag{4}$$

for the viscosity, and

$$\zeta = \frac{k_B T}{N}\frac{1}{D} \tag{5}$$

for the diffusivity. Here the term effective friction factor, $\zeta_{\text{eff}}$, is used to denote the $\zeta$ obtained by treating the copolymer as a chain of $N$ equivalent subunits, rather than $fN$ styrene and $(1 - f)N$ MMA units. In eq 4, therefore, the monomer molecular weight, $M_0$, density, $\rho$, and the statistical segment length $b$ are averaged over the composition. The degree of polymerization, $N$, is based on a constant volume corresponding to the styrene monomer. In the case of diffusion, the friction factors for PS-13* (or PS-13.5*) and PMMA-12* are "true" monomeric friction factors, whereas that for SMMA-39* is also an "effective" friction factor. A subtle but important point should be noted here. Although eq 5 should be valid for a block copolymer, with $\zeta$ thus obtained equal to the composition average of the component friction factors, the same is not necessarily true for the viscosity. The reason is that the viscosity involves the integral over the entire relaxation spectrum, and the various relaxation times can be quite strongly affected by a distribution of $\zeta$ values along the chain. This problem has been treated in some detail, both approximately[35−37] and numerically.[38] The results are complicated, but for the likely differences in component $\zeta$ occurring here, it is reasonable to assume that the error in invoking eq 4 will be less than a factor of 2.[35,38]

The friction factors thus obtained are shown in Figure 8 as a function of temperature (the units of $\zeta$ are dyn s/cm throughout). The squares correspond to homopolymers and the circles to copolymers; the filled symbols reflect viscosity-based friction factors and the open symbols those from $D$. The values of $\zeta$ from $\eta$ and from $D$ agree well, but not quantitatively; those from $D$ are systematically a little lower. We do not attribute any particular significance to this observation, given the combined uncertainties in the measured quantities and the input parameters in eq 4, plus the approximate nature of eq 4 noted above. The smooth curves represent WLF fits to the viscosity-based $\zeta_{\text{eff}}$, in this case using the glass transition temperatures from Table 2 as the reference temperatures; the associated parameter values are provided in Table 4.

The results in Figure 8 may be compared briefly with the equivalent quantities obtained for styrene−isoprene tetrablock copolymers (SISI) reported previously.[21,22] In that case the viscosity- and self-diffusion-based friction factors were in slightly better agreement with each other than is the case here. More importantly, for SISI the data extended over a much greater range in temperature (−40 to 180 °C) due to the much larger

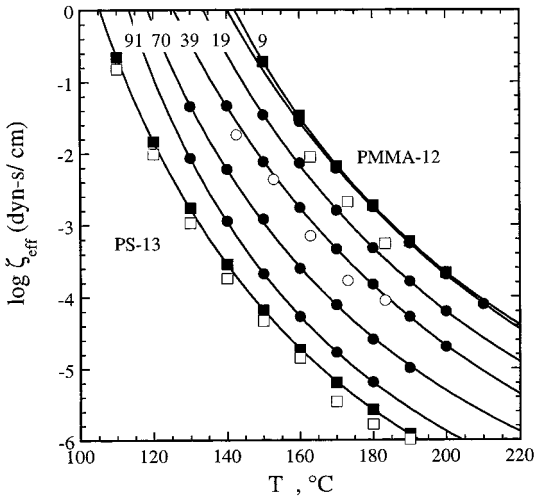


**Figure 8.** Semilogarithmic plot of the effective friction factors as a function of temperature determined from zero-shear viscosity (solid symbols) and self-diffusion (PS-13*, SMMA-39*, and PMMA-12*, open symbols). Squares indicate the result for homopolymers and circles for diblock copolymers. Solid lines indicate WLF fits to the viscosity-based data.

**Table 4. WLF Fits to the Viscosity-Based Effective Friction Factors**

| polymer | $C_1^g$ | $C_2^g$, °C | log $\zeta(T_g)$ |
|---|---|---|---|
| PS-13 | 12.69 | 85.51 | 1.635 |
| SMMA-91 | 12.82 | 106.1 | 2.371 |
| SMMA-70 | 12.89 | 89.12 | 2.300 |
| SMMA-39 | 13.57 | 95.12 | 1.893 |
| SMMA-19 | 13.63 | 66.55 | 2.320 |
| SMMA-9 | 13.69 | 55.37 | 2.188 |
| PMMA-12 | 12.65 | 63.79 | 2.328 |

difference between the $T_g$s of the components. Nevertheless, when the data were plotted against $T - T_g$ rather than $T$, they collapsed remarkably well to a single master curve, indicating that in the styrene−isoprene system the distance from the composition-dependent $T_g$ essentially determined $\zeta_{\text{eff}}$. In contrast, one can discern from Figure 8 that plotting the data against $T - T_g$ will *not* reduce the data to a master curve; for example, when $\log \zeta = -3$ the data are spread over about 50 deg whereas the difference in component $T_g$s is only 27 deg. In this sense, at least, the PS/PMMA system is more complicated than the PS/PI system. Qualitatively, this may be attributed to the relative importance of intermolecular and intramolecular constraints. For PS/PI, the former dominate; in mixtures, each component senses a common environment. For PMMA, however, the latter play a larger role; PS and PMMA are able to relax at different rates even in a common matrix.

The composition dependence of $\zeta_{\text{eff}}$ at fixed temperature is examined in Figure 9 in semilogarithmic format. The straight lines are not fits to the data but linear extrapolations between log $\zeta^0_{\text{PMMA}}$ and log $\zeta^0_{\text{PS}}$, where the superscript "0" denotes the value in the pure homopolymer. The data are rather well described in this way, and thus one can write

$$\log \zeta_{\text{eff}}(\phi, T) = \phi \log \zeta^0_{\text{PS}}(T) + (1 - \phi) \log \zeta^0_{\text{PMMA}}(T) \tag{6}$$

This particular mixing rule corresponds to that proposed by Arrhenius for the viscosity of small molecule mixtures,[39,40] which is often quite successful in that context.[41,42] However, in the spirit of the Rouse model one

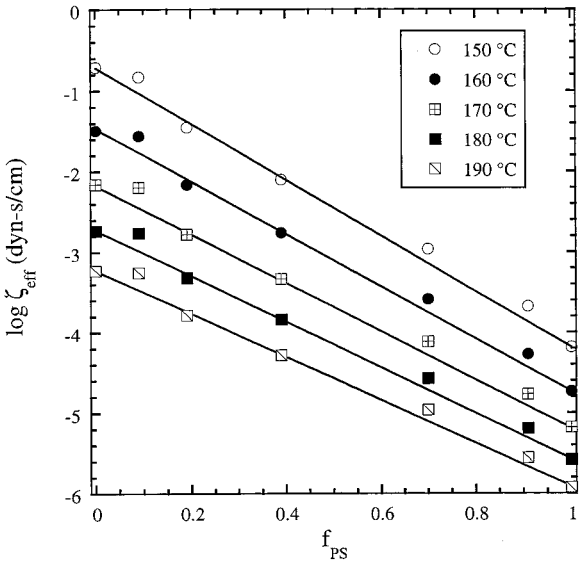


**Figure 9.** Semilogarithmic plot of the effective friction factors as a function of PS volume fraction at the indicated temperatures. Solid lines represent the Arrhenius mixing rule (eq 6).

would anticipate a different result, namely

$$\zeta_{\text{eff}}(f,T) = f\zeta_{\text{PS}}(\phi,T) + (1-f)\zeta_{\text{PMMA}}(\phi,T) \qquad (7)$$

Note that in eq 7 and henceforth we distinguish $\phi$, the *matrix* composition, from $f$, the *chain* composition, even though in Figure 9 they coincide. Equation 7 assigns a total friction factor to the chain which is a volume fraction weighted sum of the individual friction factors of the two monomers; the individual friction factors may exhibit distinct composition dependences. In contrast, the "Arrhenius" mixing rule (eq 6) gives a friction factor that is determined only by the pure component values and the composition; it corresponds to the case where the effective activation energy (or free volume, if that is the dominant feature) is a volume-weighted average of the pure component values. The apparent success of eq 6 in describing the data does not necessarily invalidate eq 7. For example, one situation where these two descriptions will coincide occurs when the individual friction factors are equal in any matrix and follow

$$\zeta_{\text{PS}}(\phi,T) = \zeta_{\text{PMMA}}(\phi,T) = [\zeta^0_{\text{PS}}(T)]^f[\zeta^0_{\text{PMMA}}(T)]^{1-f} \qquad (8)$$

i.e., the component friction factors follow the "Arrhenius" rule. The tracer diffusion measurements will permit this possibility to be assessed directly.

The component friction factors are plotted semilogarithmically in Figure 10 for PMMA (top panel) and PS (bottom panel), along with the effective friction factor for SMMA-39 (middle panel). The data for five temperatures are included as a function of matrix composition. Each set of $\zeta_{\text{PS}}(\phi)$ and $\zeta_{\text{PMMA}}(\phi)$ has been fit to straight lines, i.e., the "Arrhenius" mixing rule, and the lines have been extrapolated to the experimentally inaccessible $\zeta_{\text{PS}}(\phi=0)$ in pure PMMA and $\zeta_{\text{PMMA}}(\phi=1)$ in pure PS. The slopes for various temperatures and for the two tracers are all approximately the same, giving a 2 orders of magnitude difference between the mobilities in pure PS and in pure PMMA. The success of the linear fits for the component friction factors is consistent with the effective friction factors based on the viscosity. The monotonic decrease in $\zeta_{\text{PS}}$ and $\zeta_{\text{PMMA}}$ with increasing

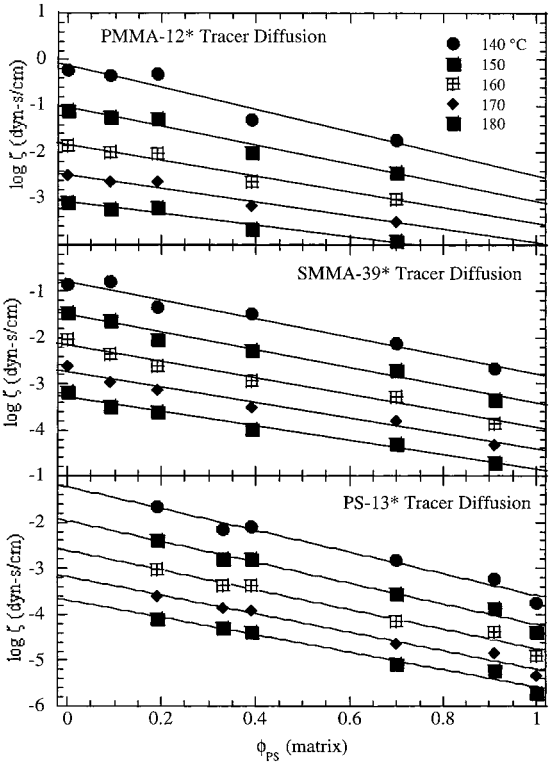


**Figure 10.** Semilogarithmic plots of the component friction factors determined from tracer diffusion of (a) PMMA-12* and (c) PS-13* in various matrices at the indicated temperatures; the data in (b) represent the effective friction factors obtained from the tracer diffusion of SMMA-39*. In all cases the straight lines represent linear regression fits.

PS content at any fixed temperature is expected on the basis of the composition dependence of $T_g$, but as noted above for $\zeta_{\text{eff}}$ (and as will be made clear subsequently), the data will not reduce to a common curve at a given $T - T_g$. The SMMA-39 effective friction factors also follow this composition dependence, which is also not surprising given the behavior of the individual components, but the magnitude of $\zeta_{\text{eff}}$ will be discussed below.

The dependence of the friction factors on tracer composition in three SMMA matrices is shown in Figure 11, again for five temperatures. In addition to the three data sets for each tracer in a given matrix, a fourth data set corresponding to $\zeta_{\text{eff}}$ for that particular matrix is included. In this case the friction factors decrease monotonically with tracer PS content in all three matrices; $\zeta_{\text{PMMA}}$ is approximately 10 times $\zeta_{\text{PS}}$ in a given matrix at any temperature. This is in marked contrast to the case of PS/PI, where $\zeta_{\text{PS}} \approx \zeta_{\text{PI}}$ in a given matrix at any temperature.[22] It is also at least qualitatively consistent with the results of Green, in that $\zeta_{\text{PMMA}}$ is significantly greater than $\zeta_{\text{PS}}$ under equivalent conditions.[23] Straight lines connecting the homopolymer values pass close to the results for SMMA-39, implying that the dependence on the tracer composition is also Arrhenius-like.

The self-diffusion data for PMMA-12 and PS-13 provide the temperature-dependent homopolymer friction factors $\zeta^0_{\text{PMMA}}(T)$ and $\zeta^0_{\text{PS}}(T)$, and the fits in Figure 10a,c provide the dependence on matrix composition:

$$\log \zeta_{\text{PS}}(\phi,T) = m_{\text{PS}}(1-\phi) + \log \zeta^0_{\text{PS}}(T) \qquad (9a)$$

$$\log \zeta_{\text{PMMA}}(\phi,T) = m_{\text{PMMA}}\phi + \log \zeta^0_{\text{PMMA}}(T) \qquad (9b)$$

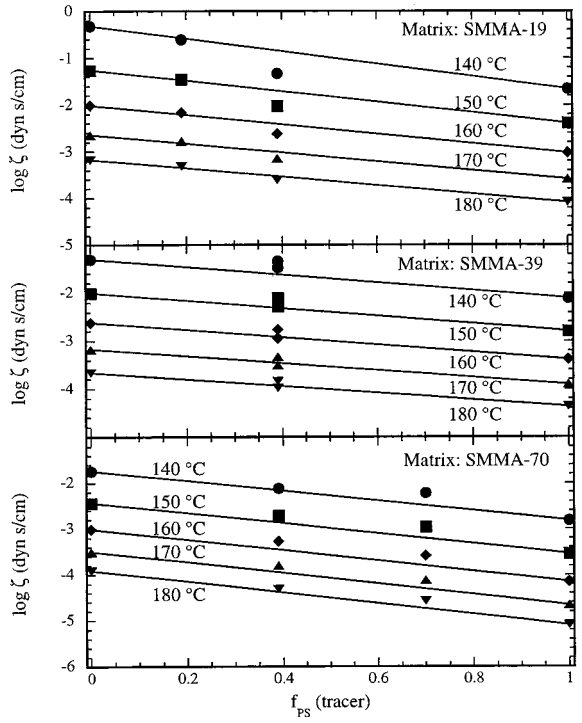


**Figure 11.** Semilogarithmic plots of the friction factors determined from tracer diffusion as a function of PS volume fraction in the tracer for (a) SMMA-19, (b) SMMA-39, and (c) SMMA-70 matrices at the indicated temperatures. Each panel also includes a set of viscosity-based effective friction factors for the matrix itself. Solid lines represent the Arrhenius mixing rule (eq 6).

**Table 5. Parameters Used To Compute $\zeta_{PS}(\phi,T)$ and $\zeta_{PMMA}(\phi,T)$ from Homopolymer Diffusion**

| parameter | PS | PMMA |
|---|---|---|
| $m$ | 2.13 | −1.79 |
| $C_1^g$ | 12.27 | 13.56 |
| $C_2^g$, °C | 55.89 | 107.5 |
| $T_g$, °C | 95.8 | 123.4 |
| log $\zeta(T_g)$ | 1.659 | 1.597 |

The values of the slopes m vary slightly with temperature, but to a reasonable approximation they are constant. The temperature dependence of the pure component values follow the WLF equation, and all the parameter values necessary to estimate either component friction factor at a given matrix composition and temperature are listed in Table 5. These values can now be used to "predict" $\zeta_{eff}(\phi,T)$ from viscosity and $\zeta_{SMMA-39}(\phi,T)$ from the copolymer tracer diffusion. The result of the first comparison is presented in Figure 12a at three temperatures. The effective friction factor data come from Figure 8, and the curves are based on eqs 9a and 9b. In particular, the two mixing rules, "Arrhenius" and "Rouse", are compared (eqs 6 and 7, respectively). Note that the curves are based on diffusion measurements, whereas the data points come from viscosity, which accounts for the slight mismatch at the composition extremes. Both mixing rules are quite successful, but if one were to shift the curves to match the data for the pure homopolymers, the "Arrhenius" rule might be preferable (as already implied by the linear interpolations in Figure 10). The comparisons of the two mixing rules with the tracer diffusion data for SMMA-39* are shown in Figure 12b. Here again both approaches work quite well. This is particularly gratifying in the case of the Rouse model, in that it provides an internal consistency check on the data; if one has the temperature and composition dependence of the component friction factors as in eqs 9a and 9b, one should be able to predict the diffusivity of any copolymer made from the two components in any matrix (i.e., eq 7).

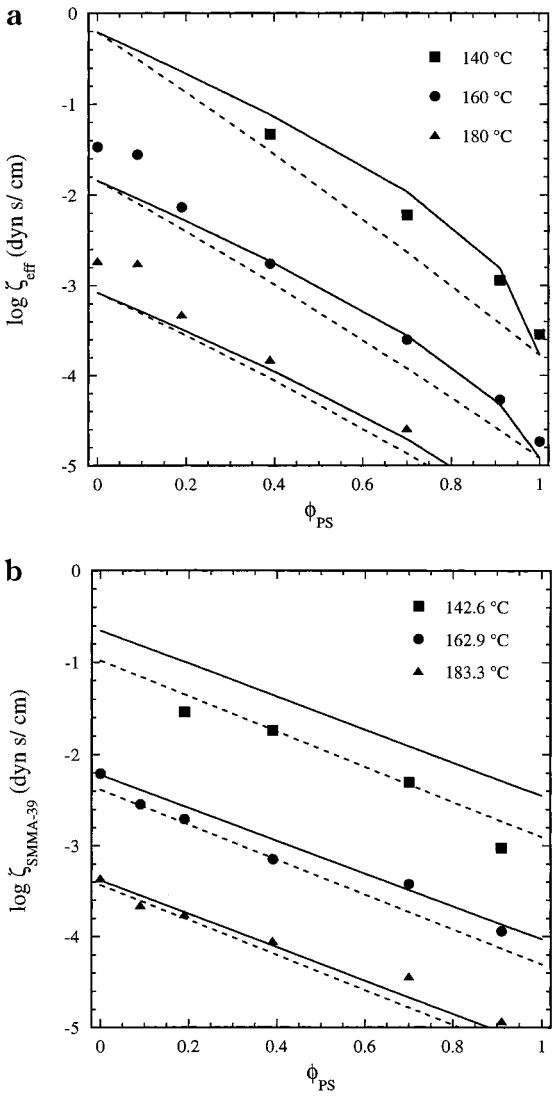


**Figure 12.** Semilogarithmic plot of the friction factor as a function of PS volume fraction in the matrix determined at the indicated temperatures: (a) effective friction factors from viscosity and (b) friction factors from SMMA-39* tracer diffusion, compared with predictions using the component friction factors from tracer diffusion and either the Arrhenius (dashed line) or Rouse (solid line) mixing rule.

To summarize the results so far, we find that (i) the pure component friction factors follow the WLF temperature dependence, (ii) the component friction factors have a composition dependence at fixed temperature given by the "Arrhenius" mixing rule, and (iii) the dynamics of a copolymer can be reliably predicted through the Rouse model given the composition and temperature dependences of the component friction factors. This behavior may be classified as relatively simple in comparison to other systems noted in the Introduction. The only obvious complexity that emerges is the fact that $\zeta^0_{PMMA}$ and $\zeta^0_{PS}$ are significantly different at either a fixed temperature (see, for example, Figure 10a,c) or at a fixed matrix $T - T_g$, as can be seen in

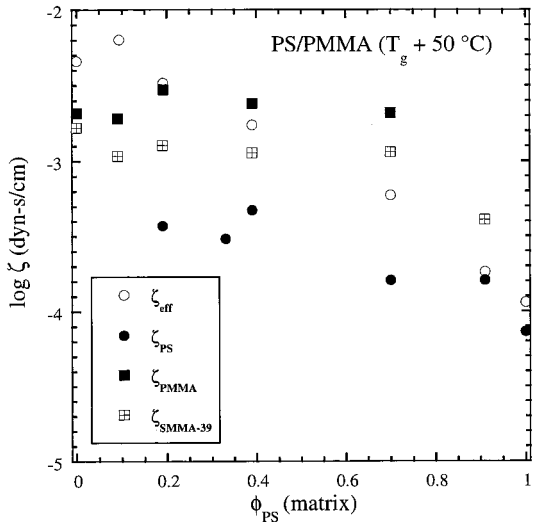


**Figure 13.** Semilogarithmic plot of the indicated friction factors as a function of the matrix composition determined at 50 °C above the matrix glass transition temperature.

Figure 13. Here we plot $\zeta_{PMMA}$, $\zeta_{PS}$, and $\zeta_{eff}$ from viscosity and $\zeta_{SMMA-39}$ as a function of matrix composition, all at a fixed 50 °C above $T_g$, via interpolation from the measured values. This format has been employed by several other workers to highlight the complexity of the results;[1,5,6] although a fixed $T - T_g$ is not, in general, an iso-free volume state, it does at least represent a reasonable reference state to consider. The first interesting feature in Figure 13 is that PMMA in PMMA is so much slower (at 174.4 °C in this case) than is PS in PS (at 145.8 °C), in agreement with past results.[18] The second is that across most of the composition range this difference is largely preserved; for example, over the composition range $0.3 \leq \phi \leq 0.7$ $\zeta_{PMMA}$ remains at least an order of magnitude larger than $\zeta_{PS}$. This implies a significant *intramolecular* contribution to $\zeta_{PMMA}$ and $\zeta_{PS}$; the two are not brought into close proximity by being placed in a common matrix. Rather, the two components retain some individual character even in the mixtures. This raises the possibility that the matrices are segregated to some extent, due to the thermodynamic interactions between PS and PMMA; in this case perhaps PMMA moves primarily though PMMA-rich regions and PS through PS-rich regions. However, we feel this contribution can be very minor at most. First, SANS measurements on the SMMA matrices revealed no hint of a structure factor peak, in contrast to the clearly defined peak in the SISI case.[21] This is consistent with the known value of $\chi$ and the chosen molecular weights. Second, the rheological properties give no hint of large-amplitude composition fluctuations, and the effective friction factors from the viscosity vary monotonically between pure PMMA and pure PS.

An alternative contributing factor is the self-concentration, $\phi_s$, as recently proposed in the context of miscible blends.[17,43] The basic concept is that any PS segment in a PS/PMMA mixture will sense a local environment that is on average rich is PS, due to chain connectivity; similarly, a PMMA segment will see a PMMA-rich local environment. Assuming the persistence length to be the relevant length scale, it was proposed that both PS and PMMA have self-concentrations of around 25%.[17] In a given matrix of bulk composition $\phi$, the average local concentrations can be estimated as

$$\phi_{eff}^{PS} \approx 0.25 + 0.75\phi, \quad \phi_{eff}^{PMMA} \approx 0.25 + 0.75(1 - \phi) \tag{10}$$

From the $T_g$ data in Figure 3, one can then estimate an effective $T_g$ as sensed by each component, based on its average local environment. For example, at an overall composition of 0.5 each component would see an effective composition of about 0.625, which would correspond to an effective $T_g$ for PS about 8 deg below the bulk value, and for PMMA about 8 deg higher, where the composition dependence of the bulk $T_g$ is used to estimate the effective $T_g$. Returning to Figure 13, by this argument the reference state of $T - T_g = 50$ °C would actually correspond to approximately $T - T_g = 42$ °C for PMMA and $T - T_g = 58$ °C for PS. Using the WLF parameters for PS and PMMA, one can "renormalize" the data in Figure 13 to $T - T_g$ (effective) = 50 °C for each component. The result is that at $\phi = 0.5$ $\zeta_{PS}$ would be increased by a factor of 2.6 and $\zeta_{PMMA}$ would be decreased by a factor of 3.5, which would bring them into near coincidence. Consequently, we conclude that the self-concentration approach can fully account for the divergence between the component friction factors in the copolymer matrices.

The remaining unexplained feature of the data is the significant difference between the pure component friction factors, i.e., between $\zeta^0_{PMMA}$ and $\zeta^0_{PS}$ at any $T$ or even $T - T_g$. As noted in the Introduction, this is not a new observation. Ferry suggested that it was tied to chemical structure through the doubly substituted backbone carbon atom, as many other polymers in this class have relatively large friction factors.[18] More recent NMR measurements on PMMA reveal a significantly anisotropic local chain motion even 50 deg above $T_g$, attributable to the large and asymmetric side chains,[44] thereby providing a more detailed molecular interpretation of Ferry's observation.

## Summary

The composition and temperature dependence of the monomeric friction factor $\zeta(\phi,T)$ has been examined in PS/PMMA matrices via measurements of viscosity and diffusion. Five SMMA diblocks of various compositions have been used. The chain lengths were such that the Rouse model should be applicable, and the order−disorder transitions were far below the experimentally relevant temperature range. Two kinds of $\zeta$ have been resolved: component friction factors, $\zeta_{PS}(\phi,T)$ and $\zeta_{PMMA}(\phi,T)$, obtained from homopolymer diffusion, and effective friction factors, $\zeta_{eff}(\phi,T)$, obtained from viscosity measurements on the copolymer matrices. The main results are as follows:

1. The values of $\zeta_{eff}(\phi,T)$ increase monotonically with MMA content at fixed temperature and with decreasing temperature at fixed composition. The composition dependence is consistent with either the Arrhenius mixing rule or one derived from the Rouse model, using only the pure component friction factors as input. The temperature dependence is consistently described by the WLF equation, but the data do not collapse to a master curve when plotted against $T - T_g$.

2. The values of $\zeta_{PMMA}(\phi,T)$ are consistently significantly greater than $\zeta_{PS}(\phi,T)$, both in their pure states at a common temperature or common $T - T_g$ or in the copolymer matrices. The difference in the pure state has been known for some time and is attributable to the specifics of the local chain relaxation dynamics in

PMMA. The differences in a common matrix can be understood in large measure through the concept of the self-concentration.

**Acknowledgment.** This work was supported by the National Science Foundation through Awards DMR-9528481 and DMR-9901087 (to T.P.L.) and by a Fellowship from Eastman Chemical Co. (J.M.M.).

## References and Notes

(1) Composto, R. J.; Kramer, E. J.; White, D. M. *Polymer* **1990**, *31*, 2320.
(2) Chin, Y. H.; Zhang, C.; Wang, P.; Inglefield, P. T.; Jones, A. A.; Kambour, R. P.; Bendler, J. T.; White, D. M. *Macromolecules* **1992**, *25*, 3031.
(3) Roovers, J.; Toporowski, P. M. *Macromolecules* **1992**, *25*, 1096, 3454.
(4) Ngai, K. L.; Roland, C. M.; O'Reilly, J. M.; Sedita, J. S. *Macromolecules* **1992**, *25*, 3906.
(5) Kim, E.; Kramer, E. J.; Wu, W. C.; Garrett, P. D. *Polymer* **1994**, *35*, 5706.
(6) Kim, E.; Kramer, E. J.; Osby, J. O. *Macromolecules* **1995**, *28*, 1979.
(7) Zawada, J. A.; Fuller, G. G.; Colby, R. H.; Fetters, L. J.; Roovers, J. *Macromolecules* **1994**, *27*, 6861.
(8) Zetsche, A.; Fischer, E. W. *Acta Polym.* **1994**, *45*, 168.
(9) Chung, G.-C.; Kornfield, J. A.; Smith, S. D. *Macromolecules* **1994**, *27*, 964.
(10) Alegria, A.; Colmenero, J.; Ngai, K. L.; Roland, C. M. *Macromolecules* **1994**, *27*, 4486.
(11) Kumar, S. K.; Colby, R. H.; Anastasiadis, S. H.; Fytas, G. *J. Chem. Phys.* **1996**, *105*, 3777.
(12) Pathak, J. A.; Colby, R. H.; Kamath, S. Y.; Kumar, S. K.; Stadler, R. *Macromolecules* **1998**, *31*, 8988.
(13) Pathak, J. A.; Colby, R. H.; Floudas, G.; Jérôme, R. *Macromolecules* **1999**, *32*, 2553.
(14) Adams, S.; Adolf, D. B. *Macromolecules* **1999**, *32*, 3136.
(15) Arbe, A.; Alegria, A.; Colmenero, J.; Hoffmann, S.; Willner, L.; Richter, D. *Macromolecules* **1999**, *32*, 7572.
(16) Kamath, S.; Colby, R. H.; Kumar, S. K.; Karatasos, K.; Floudas, G.; Fytas, G.; Roovers, J. E. L. *J. Chem. Phys.* **1999**, *111*, 6121.
(17) Lodge, T. P.; McLeish, T. C. B. *Macromolecules* **2000**, *33*, 5278.
(18) Ferry, J. D. *Viscoelastic Properties of Polymers*, 3rd ed.; Wiley: New York, 1980.
(19) Green, P. F.; Adolf, D. B.; Gilliom, L. R. *Macromolecules* **1991**, *24*, 3377.
(20) Colby, R. H. *Polymer* **1989**, *30*, 1275.
(21) Chapman, B. R.; Hamersky, M. W.; Milhaupt, J. M.; Kostelecky, C.; Lodge, T. P.; von Meerwall, E. D.; Smith, S. D. *Macromolecules* **1998**, *31*, 4562.
(22) Milhaupt, J. M.; Chapman, B. R.; Lodge, T. P.; Smith, S. D. *J. Polym. Sci., Polym. Phys. Ed.* **1998**, *36*, 3079.
(23) Green, P. F. *Macromolecules* **1995**, *28*, 2155.
(24) Allen, R. D.; Long, T. E.; McGrath, J. E. *Polym. Bull.* **1986**, *15*, 127.
(25) Freyss, D.; Rempp, P.; Benoit, H. *J. Polym. Sci., Lett.* **1964**, *2*, 217.
(26) Faldi, A.; Tirrell, M.; Lodge, T. P. *Macromolecules* **1994**, *27*, 4176.
(27) Eastman, C. E.; Lodge, T. P. *Macromolecules* **1994**, *27*, 5591.
(28) Splitter, J. S.; Calvin, M. *J. Org. Chem.* **1955**, *20*, 1086.
(29) Brandrup, J.; Immergut, E. H.; Grulke, E. A. *Polymer Handbook*, 4th ed.; John Wiley & Sons: New York, 1999.
(30) Fox, T. G *Bull. Am. Phys. Soc.* **1956**, *1*, 123.
(31) Bates, F. S.; Rosedale, J. H.; Fredrickson, G. H. *J. Chem. Phys.* **1990**, *92*, 6255.
(32) Fredrickson, G. H.; Bates, F. S. *Annu. Rev. Mater. Sci.* **1996**, *26*, 503.
(33) Fetters, L. J.; Lohse, D. J.; Milner, S. T.; Graessley, W. W. *Macromolecules* **1999**, *32*, 6847.
(34) Doi, M.; Edwards, S. F. *The Theory of Polymer Dynamics*, 2nd ed.; Clarendon Press: Oxford, 1988.
(35) Stockmayer, W. H.; Kennedy, J. W. *Macromolecules* **1975**, *8*, 351.
(36) Hall, W. F.; De Wames, R. E. *Macromolecules* **1975**, *8*, 349.
(37) Hansen, D. R.; Shen, M. *Macromolecules* **1975**, *8*, 343.
(38) Man, V. F.; Schrag, J. L.; Lodge, T. P. *Macromolecules* **1991**, *24*, 3666.
(39) Arrhenius, S. *Z. Phys. Chem. (Muenchen)* **1887**, *1*, 285.
(40) Friedman, E. M.; Porter, R. S. *Trans. Soc. Rheol.* **1975**, *19*, 493.
(41) Hirschfelder, J. O.; Curtiss, C. F.; Bird, R. B. *Molecular Theory of Gases and Liquids*; Wiley: New York, 1954.
(42) Gisser, D. J.; Ediger, M. D. *J. Phys. Chem.* **1993**, *97*, 10818.
(43) Chung, G.-C.; Kornfield, J. A.; Smith, S. D. *Macromolecules* **1994**, *27*, 5729.
(44) Schmidt-Rohr, K.; Kulik, A. S.; Beckham, H. W.; Ohlemacher, A.; Pawelzik, U.; Boeffel, C.; Spiess, H. W. *Macromolecules* **1994**, *27*, 4733.

MA010265D